HHS Public Access

Author manuscript

Pain. Author manuscript; available in PMC 2018 August 01.

Published in final edited form as:

Pain. 2017 August ; 158(8): 1461–1472. doi:10.1097/j.pain.0000000000000930.

Modulation of brainstem activity and connectivity by respiratory-gated auricular vagal afferent nerve stimulation (RAVANS) in migraine patients

Ronald G. Garcia[1,2,3], **Richard L Lin**[1,4], **Jeungchan Lee**[1], **Jieun Kim**[1,5], **Riccardo Barbieri**[6,7], **Roberta Sclocco**[1,8], **Ajay D. Wasan**[9], **Robert R. Edwards**[10], **Bruce R Rosen**[1], **Nouchine Hadjikhani**[1,11], and **Vitaly Napadow**[1,8,10]

[1]Martinos Center for Biomedical Imaging, Department of Radiology, Massachusetts General Hospital, Harvard Medical School, Boston, MA, USA

[2]Neurovascular Science Group, Fundación Cardiovascular de Colombia, Floridablanca, Colombia

[3]Connors Center for Women's Health and Gender Biology, Brigham and Women's Hospital, Harvard Medical School, Boston, MA, USA

[4]Harvard-MIT Division of Health Sciences and Technology, Harvard Medical School, Boston, MA, USA

[5]Clinical Research Division, Korean Institute of Oriental Medicine, Daejeon, Korea

[6]Department of Electronics, Information and Bioengineering, Politecnico di Milano, Milano, Italy

[7]Department of Anesthesia and Critical Care, Massachusetts General Hospital, Harvard Medical School, Boston, MA, USA

[8]Department of Radiology, Logan University, Chesterfield, MO, USA

[9]Department of Anesthesiology, University of Pittsburgh Medical Center, Pittsburgh, PA, USA

[10]Department of Anesthesiology, Perioperative and Pain Medicine, Brigham and Women's Hospital, Harvard Medical School, Boston, MA, USA

[11]Gillberg Neuropsychiatry Center, Gothenburg University, Gothenburg, Sweden

Abstract

Migraine pathophysiology includes altered brainstem excitability, and recent neuromodulatory approaches aimed at controlling migraine episodes have targeted key brainstem relay and modulatory nuclei. In this study, we evaluated the impact of respiratory-gated auricular vagal afferent nerve stimulation (RAVANS), a novel neuromodulatory intervention based on an existing transcutaneous Vagus Nerve Stimulation approach, in the modulation of brainstem activity and connectivity in migraine patients. We applied 3T-functional magnetic resonance imaging with improved in-plane spatial resolution (2.62×2.62 mm) in episodic migraine (interictal) and age- and sex-matched healthy controls to evaluate brain response to RAVANS (gated to either inhalation or

Correspondence to: Ronald G. Garcia, MD, PhD, Martinos Center for Biomedical Imaging, CNY 149-2301, 13th St. Charlestown, MA 02129, phone: 617-935-3895, rgarcia@nmr.mgh.harvard.edu.

exhalation) and sham stimulation. We further investigated RAVANS modulation of tactile trigeminal sensory afference response in the brainstem using air-puff stimulation directed to the forehead during functional magnetic resonance imaging. Compared to sham and inhalatory-gated RAVANS (iRAVANS), exhalatory-gated RAVANS (eRAVANS) activated an ipsilateral pontomedullary region consistent with nucleus tractus solitarii (NTS). During eRAVANS, NTS connectivity was increased to anterior insula and anterior mid-cingulate cortex, compared to both sham and iRAVANS, in migraine patients. Increased connectivity was inversely correlated with relative time to the next migraine attack, suggesting clinical relevance to this change in connectivity. Post-stimulation effects were also noted immediately following eRAVANS, as we found increased activation in putative pontine serotonergic (i.e. nucleus raphe centralis) and noradrenergic (i.e. locus coeruleus) nuclei in response to trigeminal sensory afference. Regulation of activity and connectivity of brainstem and cortical regions involved in serotonergic and noradrenergic regulation and pain modulation may constitute an underlying mechanism supporting beneficial clinical outcomes for eRAVANS applied for episodic migraine.

Keywords

Migraine; Transcutaneous vagus nerve stimulation; Respiratory-gated; Nucleus tractus solitarii; Functional connectivity; Raphe nuclei; Locus coeruleus

INTRODUCTION

Migraine is a prevalent (~22%) and highly disabling disorder [70]. Despite this impact, the pathophysiology of migraine remains to be elucidated [13]. Hypersensitization of the brainstem trigeminal sensory complex may underlie the primary brain dysfunction in migraine [1; 10; 58; 71], leading to brainstem-mediated upregulation of cortical excitability [14; 40]. Therapeutic options have targeted brainstem neuromodulatory centers, including serotonergic (raphe nuclei) and noradrenergic (locus coeruleus) nuclei [19; 63], via dihydroergotamine, triptans, and other 5HT1B/1D agonists [21; 41; 62]. More recently, novel neuromodulation therapies have been proposed [44; 65]. Vagus Nerve Stimulation (VNS) has demonstrated efficacy in migraine prevention and reduction of headache severity [33; 48; 80], and while the precise analgesic mechanisms of VNS are unknown, vagal afference relayed to nucleus tractus solitarii (NTS) in the medulla may modulate trigeminal sensory complex excitability and connectivity with higher brain structures [48].

Despite the therapeutic potential of VNS, adverse events associated with surgery and chronic stimulation limit broad applicability [23]. Importantly, the NTS, and spinal trigeminal nucleus (Sp5), also receive somatosensory afference via the auricular branch of the vagus nerve (ABVN) [36; 56]. Non-invasive (transcutaneous) methods of ABVN stimulation (tVNS) have been proposed [76], and preliminary neuroimaging studies have found that tVNS modulates brainstem and cortical areas similar to classical VNS [20; 24; 37], whereas a clinical trial suggested that tVNS may also reduce the frequency of migraine episodes [72].

Interestingly, the dorsal medullary vagal system operates in tune with respiration. Second-order relay neurons in the NTS receive afference from pulmonary stretch receptors and aortic baroreceptors. NTS also receives inhibitory inputs from ventral respiratory group

(VRG) nuclei in the medulla during inhalation, and facilitation during exhalation [5; 46; 47]. Our group has proposed that ABVN stimulation gated to exhalation may optimize tVNS [53].

Brainstem functional magnetic resonance imaging (fMRI) methods have begun to address the inherent difficulties in imaging this subcortical structure. The brainstem is especially prone to physiological noise, and its proximity to the steep magnetic susceptibility gradient from the air-tissue boundary with the oral cavity leads to magnetic-field inhomogeneities. Moreover, the small cross-sectional area of brainstem nuclei requires enhanced spatial resolution compared to conventional brain-focused fMRI [6]. With such caveats in mind, imaging studies have shown interictal abnormalities in migraneurs in subcortical and brainstem regions responsible for somatosensory processing [2; 30; 45; 49; 50]. For instance, our recent fMRI study found that Sp5 response to tactile stimuli in migraine was amplified in higher cortical regions and sensitive to interictal phase [40]. Neuromodulatory interventions, such as tVNS, can target specific brainstem nuclei and the trigeminal sensory pathway to ameliorate migraine pathophysiology and reduce headache frequency and severity.

In this study we applied fMRI to evaluate brainstem response to Respiratory-gated Auricular Vagal Afferent Nerve Stimulation (RAVANS) in interictal migraine patients. We also investigated RAVANS modulation of brainstem response to tactile stimulation along the trigeminal pathway. We hypothesized that compared to sham stimulation (SHAM), exhalatory-gated RAVANS (eRAVANS) will more effectively target NTS, and modulate NTS-cortical connectivity and trigeminal sensory processing in brainstem neuromodulatory (e.g. serotonergic, noradrenergic) nuclei. An exploratory analysis then compared brain response to eRAVANS versus inhalatory-gated RAVANS (iRAVANS).

METHODS

Study Population

Sixteen migraine patients (MIG, 15 females, 35.8 ± 13.4 years old, mean ± SD) and sixteen sex-/age-matched healthy control subjects (HC, 15 females, 36.0 ± 13.7 years old, $p = 0.96$) participated in this study (Table 1). Patients were diagnosed with episodic migraine based on classification of the International Headache Society [32]. Seven patients (43.7%) were diagnosed with migraine with aura and none suffered from any other major neurological or psychiatric disorders. Subjects completing this study were not prescribed opioids, benzodiazepines, or cannabinoids, however 7 subjects were receiving prophylactic medications (Table 2). Only migraine patients with uncomplicated cases of 2–15 attacks per month were enrolled. Healthy control subjects had no history of primary headache or other pain syndromes. All studies were performed at the Martinos Center for Biomedical Imaging in Boston, Massachusetts. The experimental procedure was approved by the Partners Human Research Committee, and all research participants were fully informed and gave written informed consent to participate in the study.

Clinical Characterization

In migraine patients, clinical characterization included assessment of self-reported episodes per month and time since diagnosis. All migraine patients were scanned interictally (i.e. between episodes). Subjects were asked on the day of the MRI scan the time since the presentation of their preceding ictal event (PRE_I: number of days between previous migraine episode and MRI scan visit), and were followed up by phone to collect information about their subsequent migraine episode after the scan visit (NEXT_I: number of days between MRI scan visit and subsequent migraine episode). An "interictal phase index" was then calculated (see equation 1) to take into account variability in individual patients' episode-to-episode cycle, resulting in a metric scaled from 0 (immediately after last attack) to 100 (immediately preceding next attack). This index has some advantages over other measurements such as the number of days after or preceding an attack, because it takes into account the variability of attack frequency between patients, normalizing the time since last attack by the total duration of the interictal period. This measurement has been previously shown by our group to correlate with fMRI activation in brainstem trigeminal nuclei in response to ophthalmic nerve somatosensory input [40], and our current analysis explored whether the interictal phase index is also sensitive to brainstem processing of RAVANS stimulation.

Equation 1
Calculation of Interictal Phase Index

$$INTERICTAL\,PHASE = \frac{PRE\_I}{PRE\_I + NEXT\_I} * 100$$

Study Design

All subjects attended one scanning session and completed a cross-over design fMRI experiment which was composed of multiple fMRI scan runs. Two stimulation scan runs (eRAVANS, duration = 360 seconds; SHAM, electrode setup but no stimulation, duration = 360 seconds), were completed with randomized order. Before and after each stimulation scan run, subjects experienced an air-puff stimulation scan run (Air-puff pre, duration = 370 seconds; Air-puff post, duration = 370 seconds). Structural MRI scans were acquired between the cross-over for these two experimental fMRI scan sequences (wash-out interval = 30 minutes). At the end of this sequence, an iRAVANS (iRAVANS; duration = 360 seconds) scan run was performed as an exploratory comparison to eRAVANS stimulation (Figure 1). This comparison was deemed exploratory as stimulation order between eRAVANS and iRAVANS was fixed and not counterbalanced (see Limitations section of the Discussion).

Air-puff stimulation

To investigate the effects of eRAVANS on input directed along the trigeminal sensory pathway, we evaluated stimulus-evoked fMRI brainstem response to an innocuous somatosensory (air-puff) stimulation over a trigeminal nerve area. For both migraine patients and healthy controls, MR-compatible air tubing (inner diameter = 12 mm) was positioned

over the right supraorbital region of the forehead (ophthalmic (V_1) spinal trigeminal nerve branch, Figure 2A). The tubing was passed through the MR-scanner penetration panel and connected to an air compressor controller (AIRSTIM, San Diego Instruments, Inc., San Diego, CA) located outside the scanner. Air-puff stimulation (80 Psi, 5 Hz) was delivered to the subjects using a block design (14-seconds ON and 20-seconds OFF, 11 repetitions, total: 370 seconds) (Figure 2B). After the fMRI experiment, the intensity of air-puff sensations was rated by subjects on a numerical rating scale (NRS) of 0 to 10 (0: no sensation, 10: pain detection threshold, i.e. on the verge of painful sensation). Differences in air-puff ratings after RAVANS (Air-puff post vs. Air-puff pre) were evaluated according to GROUP (MIG, HC) and the type of STIMULATION (eRAVANS, SHAM). These comparisons were performed using a two-way ANOVA followed by post-hoc testing (STATA 14, Stata Corporation, College Station, TX). Our previous study [40] found altered trigeminal air-puff processing in MIG, and the current study investigated how eRAVANS affects brainstem response to such trigeminal input.

Respiratory-gated Auricular Vagus Nerve Stimulation (RAVANS)

For RAVANS setup, two MRI compatible electrodes (8mm diameter, Astro-Med, Inc, West Warwick, RI) were placed in the auricle of the left ear, fixed in place by a custom-designed plastic armature that wrapped around the ear. Auricular locations were (1) the cymba concha and (2) the slope between the antihelix and cavum concha (Figure 3). These locations were chosen based on auricular subregions with the greatest probability of vagal innervation of the human auricle, as determined by cadaver dissection [61]. Electrodes were passed through the penetration panel with inline low-pass RF filtering (80 MHz). Electrical stimulation to these electrodes was provided by a current-constant stimulator (S88X GRASS stimulator, Astro-Med, Inc, West Warwick, RI). Stimuli consisted of rectangular pulses with 450 μs pulse width, delivered at 30 Hz, and pulse train duration of 0.5 seconds, similar to our prior eRAVANS study in chronic pain patients [53]. Stimulation was gated, with 0.5-second delay, after peak inhalation (i.e. during exhalation, for eRAVANS) or after peak exhalation (i.e. during inhalation, for iRAVANS).

Respiratory gating for stimulation required real-time evaluation of the respiratory cycle. We used a MR-compatible belt system constructed in-house, based on the system devised by Binks et al. [9], and similar to the system used in several of our previous studies [35; 52]. A pneumatic belt was placed around the subject's lower thorax. Low-compliance tubing connected this belt to a pressure transducer (PX138-0.3D5V, Omegadyne, Inc., Sunbury, OH), thereby producing voltage output that corresponded to changes in respiratory volume. The voltage signal from the transducer was acquired by a laptop-controlled device (National Instruments DAQ USB-6009, 14bit i/o, with Labview 7.0 data acquisition software, Austin, TX). Computer code detected peak-inspiration and peak-expiration in real-time and a TTL signal was output to a miniature high-frequency relay (G6Z-1P-DC5, Omron Electronics Components, Schaumburg, IL) in order to open the gate and allow electrical stimulation to pass to the subject. Correct exhalatory- and inhalatory-cycle stimulation was confirmed by the experimenter via real-time inspection of respiration and stimulation signals on a graphical chart display programmed with our custom Labview software code. Post-hoc review of these tracings was also performed to confirm accurate stimulation.

Once electrodes were set up, subjects were asked to rate stimulation intensity on an NRS of 0 to 10 (0:no sensation, 10: pain detection threshold). Current intensity was set to achieve moderate to strong (but not painful) sensation (NRS target score: 5/10), and this current intensity was used on subsequent stimulation runs. For SHAM stimulation, the electrodes in the ear remained in place, but the leads were disconnected from the stimulator. Subjects were instructed that for this fMRI scan run they may or may not feel pulsing in their ear, and that we wanted to ensure that the stimulus was not painful.

MRI and Physiological Data Collection

All fMRI scans were collected using a 3T MRI scanner (Trio, Siemens Medical, Germany) equipped with a 12-channel head coil. Subjects were instructed to relax and lay supine in the scanner with their eyes closed while staying alert and awake. They were also asked to not move their head and focus on the sensation experienced on the forehead (air-puff) or ear (RAVANS) during functional scan runs. Earplugs were provided to attenuate noise during data collection.

High-resolution ($1\times1\times1mm^3$ voxels) structural MRI scans were acquired with a standard T1-weighted MP-RAGE pulse sequence (TR=2530 ms, TE=1.64 ms, flip angle= 7°, FOV=256×256 mm^2) and contained 176 axial slices. Whole brain fMRI data were acquired using a T2*-weighted blood oxygenation level dependent (BOLD) pulse sequence with increased matrix size to enable relatively improved in-plane spatial resolution and increase sensitivity to localize brainstem nuclei with small cross-sectional area (TR=2500 ms, TE=30 ms, flip angle=90°, FOV=220×220 mm^2, matrix=84×84, 43 axial slices, slice thickness=2.62 mm, gap=0.5 mm, voxel size=2.62×2.62×3.12 mm^3).

Peripheral physiological data (e.g. respiration volume, cardiac pulse pressure) were acquired using the Powerlab system (ML880, ADInstruments Inc., Colorado Springs, CO) at a 400 Hz sampling rate. In addition to the respiration volume signal noted above, cardiac pulsatility data were acquired using a piezoelectric pulse transducer (AD Instruments Inc., Colorado Springs, CO) attached to the right index finger.

MRI Data Pre-processing

Functional MRI data were pre-processed using the validated FMRIB software library (FSL) version 5.0 (http://www.fmrib.ox.ac.uk/fsl) [78], Analysis of Functional NeuroImages (AFNI) (afni.nimh.nih.gov/afni) and FreeSurfer (http://surfer.nmr.mgh.harvard.edu/) software packages. For each scan, pulse traces and respiration signals were resampled at 40 Hz, and were used for physiological noise correction using AFNI's RETROICOR function [26]. Cardiac pulse annotation was performed using an automated method followed by manual confirmation, while respiratory volume per time was calculated using an automated algorithm and custom-made MATLAB scripts (The MathWorks Inc., Natick, MA). Functional data underwent motion correction using FSL-MCFLIRT [34], and skull removal was performed using FSL-BET [69]. The fMRI data were spatially smoothed using a Gaussian kernel of full width at half maximum (FWHM) 5 mm, and temporally high-pass filtered (f=0.0147 Hz). Structural MRI data were registered to fMRI data using boundary-based registration (Freesurfer, bbregister [28]), followed by co-registration of the structural

data to standard space (MNI152) template using non-linear warping (FNIRT) [3], with the resultant transform applied to the functional parameter estimates calculated in the first-level analysis.

MRI Data Analysis

Brainstem response to RAVANS—A first-level event-related general linear model (GLM) was performed with the FMRI Expert Analysis Tool (FEAT, FSL) to estimate brainstem response to RAVANS and SHAM stimulation. The explanatory variable was defined with a text file of the electrical stimuli onset and duration convolved with the canonical hemodynamic response function (Double-Gamma). The results of this first-level analysis (i.e., parameter estimate and its variance) were transformed into standard space (MNI152), and submitted to group analyses (Randomise, FSL) using permutation-based nonparametric tests (5000 permutations) with voxel-based correction for multiple comparisons ($p < 0.05$) [31; 54]. A brainstem mask, defined by thresholding the Harvard-Oxford Subcortical Structural Atlas brainstem label at 20%, was used to spatially restrict this analysis. Group activation was calculated for a combined sample from both the MIG and HC groups in order to maximize SNR for brainstem response to the auricular stimulation and to define regions-of-interest (ROIs) with unbiased localization for subsequent analyses.

After contrasting eRAVANS versus SHAM stimulation, a ponto-medullary cluster consistent with purported left NTS (based on the Duvernoy brainstem atlas [51], see Results) was found. An exploratory analysis then contrasted eRAVANS with iRAVANS, using data (mean percent signal change of activated voxels) taken from a 3-mm radius sphere mask centered on the peak activation voxel from this cluster. A Shapiro-Wilk test was used to evaluate normality of the distribution of data, and comparisons were performed with appropriate statistical test (e.g. paired t-test).

Functional connectivity response to RAVANS—Functional connectivity was computed using seed-based correlation analysis [27]. The seed was defined based on the previously described NTS-ROI (peak MNI voxel coordinates [X, Y, Z; mm]: −8, −38, −42 with 3 mm radius). Specifically, the extracted fMRI time series from this seed was used as a GLM regressor (FEAT, FSL) for eRAVANS and SHAM data. Nuisance regressors included fMRI signals from deep cerebral white matter and cerebral ventricles using previously validated masks [75]. Notably, we did not include the global fMRI signal in this GLM. Resultant whole-brain parameter estimates, and their variance, from each individual were passed up to group-level analyses to evaluate NTS connectivity differences between eRAVANS and SHAM stimulations, for both MIG and HC, using FMRIB's Local Analysis of Mixed Effects (FLAME 1+2). The results were thresholded using cluster correction for multiple comparisons ($Z > 2.3$, cluster-size threshold of $p < 0.05$). For further exploratory analyses with i-RAVANS, functional connectivity values from significant clusters' peak voxels were used for ROI comparisons.

We then performed correlation analyses to investigate the link between purported NTS connectivity (eRAVANS – SHAM change score from analysis above) and clinical measures such as interictal phase index, number of migraine episodes per month, and duration of the

disease. After testing for normal distribution, a Pearson's correlation coefficient, *r*, was calculated, significant at $p < 0.05$.

RAVANS modulation of brainstem response to air-puff stimulation—Brainstem responses to air-puff stimulation, collected in pre- and post-RAVANS runs, were calculated in a first-level GLM analysis (FEAT, FSL) using a regressor for air-puff stimulation. The results of this analysis were submitted to non-parametric permutation analysis (Randomise, FSL) to evaluate the effects of RAVANS on the modulation of brainstem response to air-puff stimulation (two-sample paired *t*-test: Air-puff post-RAVANS vs. Air-puff pre-RAVANS, analysis procedure similar to the RAVANS brainstem activation analysis above). Significant voxels from the above analysis were used to calculate mean percent signal change in order to perform an ANOVA with factors GROUP (MIG, HC) and STIMULATION (eRAVANS, SHAM), followed by post-hoc testing (STATA 14, Stata Corporation, College Station, TX).

RESULTS

Demographic characteristics and clinical features of migraine patients are presented in Table 1. Migraine subjects with aura did not differ from others in terms of average number of episodes per month (5.9±2.1 vs 5.9±3.1, p=0.98), migraine duration (14.3±15.1 years vs 15.4±12.0 years, p=0.87), or interictal phase index (66.4±21.6 vs 60.5±31.9, p=0.68).

All subjects tolerated the air-puff procedures and auricular electrical stimulation, and both were rated as non-painful (below 10, "on the verge of being painful," on the 0–10 NRS). There were no group differences between HC and MIG in average electrical current intensity during eRAVANS or iRAVANS (Table 1). There were no differences in the number of breaths taken during SHAM compared to eRAVANS (SHAM: 92.9±16.5 vs eRAVANS: 90.9±16.1, p=0.21) or eRAVANS compared to iRAVANS (90.9±16.1 vs 92.4±16.1, p=0.39). We again found no differences between HC and MIG for these variables (Table 1). Subject ratings of air-puff stimulation intensity, after versus before RAVANS (air-puff post vs air-puff pre) did not show a significant GROUP (F=0.01, p=0.93), STIMULATION (F=0.01, p=0.93) or STIMULATION by GROUP interaction (F=0.19, p=0.66).

Brainstem response to RAVANS

No subjects were removed from analysis due to excessive head motion during RAVANS stimulation, which did not differ between groups during eRAVANS (MIG: 0.09±0.07 mm, HC: 0.08±0.06 mm, p=0.59), iRAVANS (MIG: 0.10±0.05 mm, HC: 0.10±0.08 mm, p=0.81) or SHAM (MIG: 0.09±0.08 mm, HC: 0.08±0.05 mm, p=0.74). When contrasting eRAVANS and SHAM stimulation across all subjects, permutation analysis revealed activation of a small cluster in the pontine-medullary junction (peak MNI voxel coordinates [X, Y, Z; mm]: −8, −38, −42, obex+18 mm, using verticalized brainstem coordinate), consistent with purported NTS (Table 3a, Figure 4).

To evaluate potential order effects of the stimulation due to our cross-over design, we performed an ROI analysis contrasting purported NTS response to eRAVANS for subjects randomized to having eRAVANS first in order (i.e. before SHAM stimulation) versus those randomized to having eRAVANS second in order (i.e. after SHAM stimulation). This

analysis found no significant differences in NTS BOLD %-signal response to eRAVANS when delivered first versus second in order (1.08±0.45 % vs 0.88±0.53 %, p=0.77), suggesting that the order of stimulation did not have a significant effect on NTS response. We then performed an exploratory paired t-test which showed a significant greater NTS BOLD %-signal change during eRAVANS compared to iRAVANS (0.93±0.35 % vs −0.09±0.43%, p=0.02).

Functional brain connectivity response to RAVANS

We used the purported NTS activation reported above as a seed for whole-brain functional connectivity analyses. When contrasting eRAVANS versus SHAM in all subjects, we did not see a significant difference. However, in MIG subjects alone during eRAVANS, compared to SHAM, NTS connectivity was increased to left anterior insula (aIns), anterior mid-cingulate cortex (aMCC)/pre-supplementary motor area (pre-SMA, with some spread to SMA) (Table 3b, Figure 5A). We also analyzed differences in seed functional connectivity according to order of stimulation and did not find significant differences in NTS connectivity values to aIns (0.81±0.95 vs 0.71±0.95, p=0.75) or aMCC (0.93±1.45 vs 0.14±1.39, p=0.12) when comparing subjects randomized to having eRAVANS first in order versus those randomized to have eRAVANS after SHAM stimulation. A further exploratory ROI analysis revealed greater NTS connectivity to aIns (0.9±0.29 vs 0.02±0.32, p=0.03) and aMCC (1.09±0.33 vs 0.01±0.39, p=0.04) in MIG during eRAVANS administration compared to iRAVANS stimulation.

We then evaluated potential links between these brain responses and MIG clinical variables of interest. For the evaluation of purported NTS connectivity correlations with interictal phase index, two subjects who were scanned shortly after or before a migraine attack (interictal phase index of 4 and 100) were excluded, as the peri-ictal period may differentially modulate functional connectivity [66]. We found a significant negative correlation between NTS connectivity (eRAVANS vs. SHAM) to aIns (r=−0.83, p=0.0003) and aMCC (r=−0.76, p=0.001) with the interictal phase index (Figure 5B). This association was also present if the two peri-ictal phase subjects were included in the analysis (aINS: r=−0.80, p=0.0002; aMCC: r=−0.54, p=0.02). Thus, MIG patients who were closer to their next migraine attack showed a reduced increase in connectivity in response to eRAVANS. No significant correlations were found to any other clinical variables.

RAVANS modulation of brainstem response to air-puff stimulation

For air-puff stimulation scans, no subjects were removed from analysis due to excessive head motion, and average displacement did not differ between MIG and HC (RMS displacement: 0.11±0.09 mm and 0.11±0.05 mm, respectively, p=0.91). When contrasting Air-puff post- vs. Air-puff pre-eRAVANS stimulation in all subjects (MIG plus HC), we did not see any significant difference. However in MIG patients alone, permutation analysis revealed a significantly increased activation in small clusters in the upper pons consistent with nucleus raphe centralis (peak MNI voxel coordinates [X, Y, Z; mm]: 0, −36, −28, obex +32 mm, using verticalized brainstem coordinate) and left locus coeruleus (peak MNI voxel coordinates [X, Y, Z; mm]: −4, −36, −26, obex+34 mm, using verticalized brainstem coordinate) (Table 3c, Figure 6). We further interrogated these results by performing a 2×2

ANOVA with both STIMULATION (eRAVANS, SHAM) and GROUP (MIG and HC) factors, and a significant STIMULATION by GROUP interaction for both nucleus raphe centralis (F=6.59, p=0.01) and locus coeruleus (F=3.99, p=0.04) was found. Post-hoc analyses showed a significant increase in activation of these nuclei to air-puff stimulation for MIG after eRAVANS vs SHAM compared to HC (Figure 6).

DISCUSSION

Our fMRI results show that exhalatory-gated RAVANS (eRAVANS) effectively activates a pontomedullary nucleus consistent with purported ipsilateral (left) NTS. Activation was stronger for exhalatory-gated, compared to SHAM stimulation and inhalation-gated RAVANS. Furthermore, during eRAVANS in episodic migraine patients, functional connectivity was increased between NTS and anterior insula, aMCC and preSMA, regions known to be involved in pain experience and/or regulation. Increased connectivity was inversely correlated with relative time to the next migraine attack, which might suggest clinical relevance to this change in connectivity. Post-stimulation effects were also noted, immediately after eRAVANS. Specifically, we found increased activation in putative pontine serotonergic (i.e. nucleus raphe centralis), and noradrenergic (i.e. locus coeruleus) brainstem nuclei in response to trigeminal sensory afference, after eRAVANS. These results support a neurophysiological model by which tVNS in general, and eRAVANS in particular, may modulate brain processing in episodic migraine.

Our group has previously proposed that ABVN stimulation gated to exhalation may optimize tVNS [53]. Previous studies have shown that the NTS receives (1) afference from pulmonary stretch receptors and aortic baroreceptors, (2) inhibitory inputs from ventral respiratory group (VRG) nuclei in the medulla during inhalation, and (3) facilitatory inputs during exhalation [5; 46; 47]. Exhalatory stimulation, when NTS is not receiving inhibitory VRG influence, may thus enhance NTS-mediated modulation of upstream brainstem and cortical circuitry involved in pain regulation. Furthermore, by supplying afference with intermittent, naturally irregular stimulation, respiratory-gated tVNS may limit the neural habituation occurring with repeated stimulation over tens of seconds or even minutes, common with most VNS and tVNS applications [82].

A preliminary study has suggested a potential therapeutic effect of tVNS in migraine [72], however the mechanisms underlying such focused somatosensory afference therapy have not been elucidated. Imaging studies have shown interictal abnormalities in migraineurs in subcortical and brainstem regions supporting somatosensory processing [2; 30; 45; 49; 50]. These regions might also modulate activity in non-somatosensory regions that regulate the wide range of symptoms characteristic of migraine, such as yawning, nausea, fatigue, craving and motor clumsiness, allodynia, photophobia, phonophobia, osmophobia and irritability [2; 59]. More specifically, the NTS in the dorsal medulla of the brainstem is the recipient of most afferent vagal fibers, including the ABVN [56], and is an important processing relay center for a variety of vital functions. Studies indicate that the rostral segment of the NTS sends axons to the facial, trigeminal, and hypoglossal nuclei, whereas the caudal segment sends axons to efferent (premotor) parasympathetic nuclei, including the dorsal motor nucleus of the vagus (DMNX) and nucleus ambiguus (Namb) [57]. Our results

suggest activation of the rostral NTS segment, supporting a potential modulatory effect on trigeminal sensory complex pathways. This is in line with previous animal studies reporting that invasive direct vagal stimulation suppresses Sp5 response to noxious stimulation of the face [12] or dura [43].

Although the area activated by eRAVANS is consistent with NTS according to the commonly-used brainstem atlas [51], it is possible that stimulation also activated Sp5, which is located just ventral to NTS. In fact, previous animal studies using horseradish peroxidase (HRP) applied to auricular branch of the vagus nerve have demonstrated labeling in both NTS and Sp5 [56]. However, our previous fMRI study in MIG subjects found that somatosensory stimulation over the right forehead in the ophthalmic nerve (V_1) trigeminal territory also produced activation in a pontomedullary junction cluster, but was more cranial and ventrolateral compared to the cluster noted in response to eRAVANS, and more consistent with atlas definitions of Sp5 [40].

Importantly, NTS also transfers information to monoamine nuclei in the brainstem such as locus coeruleus (noradrenergic) and raphe (serotonergic) nuclei [57; 74]. Our results showing brainstem activation immediately after eRAVANS suggest that this intervention may increase the response of putative raphe nuclei to tactile stimulation over the ophthalmic trigeminal nerve area. The raphe nuclei play an important role in the release of serotonin in the central nervous system and anti-nociceptive processing [77]. These nuclei are part of a descending pain inhibitory system, which also receives strong inputs from the cortex [60], and animal experiments have shown that raphe activation can modify nociceptive input at the level of Sp5 [16]. Moreover, raphe activity can be modulated by common migraine medications [22], suggesting a pivotal role of these nuclei in the therapeutic response to pharmacotherapy in migraine.

Based on our results, we further hypothesize that eRAVANS increases response in locus coeruleus to tactile stimulation of the trigeminal sensory pathway. The locus coeruleus is the main source of noradrenaline production in the brain with connections to cortical structures and to the spinal cord dorsal horn [42]. This nucleus also inhibits nociceptive processing in the sensory trigeminal nucleus and Sp5 [18], similar to raphe nuclei. In addition, locus coeruleus could be involved in vascular regulation of migraine through direct projections to both intra- and extra-cranial vasculature [39]. As previously discussed with NTS and Sp5, locus coeruleus is also located just medial to another structure related with trigemino-sensory afference, the mesencephalic trigeminal nucleus (MTN) [51]. This nucleus has been involved in the processing of proprioceptive signals of the face [73]. Thus, our cluster may also include MTN. If so, eRAVANS may have the potential to regulate abnormal trigeminal somatosensory/proprioceptive processing, which could also have implications for migraine therapeutics.

Another possible mechanism for the effects of eRAVANS may stem from serotonergic and noradrenergic suppression of cortical spreading depression [63], a slowly propagating wave of sustained strong neuronal and glial depolarization that underlies migraine aura and activates downstream inflammatory and nociceptive pathways [4]. Indeed, previous animal studies [17] have shown that non-invasive transcutaneous and invasive direct vagus nerve

stimulation significantly suppress cortical spreading depression susceptibility in the occipital cortex in rats. In sum, our results suggest that eRAVANS has the potential to affect key pathophysiological migraine mechanisms via noradrenergic and serotoninergic pain inhibitory pathways that down-regulate trigeminal hypersensitization and suppress cortical spreading depression.

Our results in migraine patients also found increased purported NTS connectivity to anterior insula and mid-cingulate cortex during eRAVANS, regions notably involved in the pathophysiology of migraine [11; 29]. The NTS is known to send monosynaptic projections to higher brain regions such as the parabrachial nucleus, ventromedial medulla, periaqueductal gray, anterior cingulate and lateral prefrontal cortex [8; 64] - regions hypothesized to support VNS therapeutic effects [81]. Altered connectivity in these pain-processing regions has been noted in interictal migraine patients [25; 29; 55; 67; 79]. Abnormalities in insula connectivity are of particular relevance, given that this region integrates multimodal afference from somatosensory, nociceptive and visceral streams with activity in prefrontal cortex, limbic structures, and olfactory, visual and auditory processing regions [11]. Reduced functional connectivity between anterior insula and occipital lobe areas has been reported in interictal migraine patients with aura compared with healthy controls [55], whereas other studies have demonstrated increased connectivity between bilateral amygdala and anterior insula in interictal migraine patients [29]. The anterior insula together with cingulate cortex is involved in the processing of stimulus salience [68] and the affective/emotional components of nociception [38]. These regions also participate in the integration and regulation of autonomic responses to pain [7; 15]. Future studies should evaluate whether the effects of eRAVANS on NTS connectivity to anterior insula and cingulate cortex is directly linked to improved autonomic symptomatology and/or reduced autonomic response to nociception in migraine patients.

Finally, we found an inverse relationship between increased NTS connectivity to insula and cingulate cortices and relative time to next migraine attack (greater interictal phase index). Our prior study supported the clinical relevance of the interictal phase index, as Sp5 response to trigemino-sensory afference was associated with this index [40]. The observed increased association in the present study may reflect a beneficial response as (1) connectivity is reduced as patients approach their next attack, and (2) healthy controls demonstrate increased NTS-insula connectivity in response to eRAVANS compared to SHAM. If increased connectivity is indeed beneficial, it would suggest that the use of eRAVANS might have improved clinical effects if applied relatively *early* after patients' previous attack, with repeated applications aimed at maintaining this elevated connectivity response. Furthermore, this effect might also be associated with other clinical variables such as pain intensity, however, further longitudinal studies with neuroimaging and clinical evaluation will be needed to evaluate these hypotheses. Interestingly, closer inspection of the correlation plot suggests that the connectivity to interictal phase association may not be linear as connectivity may still be reduced at relatively low (<20) interictal phases (i.e. close to prior migraine attack). This lagged response may reflect the potential for multi-day durations of the migraine attack in some patients and/or delay in neurophysiological recovery from the prior attack.

Several limitations to our study should be mentioned. Although clinical measures were not different between migraine patients with and without aura, our sample size did not allow for direct comparisons of fMRI measures between these subgroups. In the present study, our main aim was to evaluate the effects of eRAVANS vs SHAM in the modulation of brainstem activity and connectivity of MIG patients, however we also included exploratory comparisons with inhalatory-gated stimulation in order to identify the specificity of RAVANS effects to each respiratory phase (exhalation/inhalation). Given that the order of iRAVANS was not counterbalanced relative to eRAVANS, potential order confounds may have affected our results. While we cannot rule out these effects, our results showing no significant differences in NTS response to eRAVANS when delivered before or after SHAM suggest that the order of stimulation did not have a significant impact. As another limitation, we only observed activation of rostral NTS in response to eRAVANS and not of other NTS segments such as interstitial, dorsal and commissural subnuclei. This lack of activation may have been due to the small cross-sectional area of the NTS, and future studies using ultrahigh field (e.g. 7T) fMRI, with better SNR and spatial resolution, should be performed.

In conclusion, our data suggest that RAVANS, particularly eRAVANS, activates NTS and is associated with greater NTS connectivity to brain areas known to be involved in pain regulation in migraine patients. In fact, increased purported NTS connectivity to insula and cingulate cortex was correlated with interictal phase of migraine episodes, suggesting optimal timing for initiation of RAVANS therapy and a potential mechanistic target. In addition, our results suggest that eRAVANS modulated brainstem raphe nuclei and locus coeruleus response to somatosensory afference over the ophthalmic trigeminal nerve. This suggests modulation of serotoninergic and noradrenergic pain inhibitory pathways. Future studies should evaluate the longitudinal effects of RAVANS, linking stimulus-evoked brainstem response to meaningful long-term clinical outcomes in migraine.

Acknowledgments

We would like to thank Hanhee Jung for assistance in recruitment and scanning. This study received support by the National Institute of Health (NIMH R21-MH103468, NCCIH: P01-AT006663, R01-AT007550; NIAMS: R01-AR064367; NINDS R21-NS082926; NIH Office of the Director: OT2-OD023867; NHLBI-NIH U54HL119145 to Vitaly Napadow); the American Heart Association (16GRNT26420084); and the Colombian Department of Science, Technology and Innovation (COLCIENCIAS, Grant No. 65664239871). The authors declare no potential conflicts of interest with respect to the research, authorship, and/or publication of this article.

References

1. Abanoz Y, Abanoz Y, Gunduz A, Savrun FK. Trigeminal somatosensorial evoked potentials suggest increased excitability during interictal period in patients with long disease duration in migraine. Neurosci Lett. 2016; 612:62–65. [PubMed: 26644335]
2. Akerman S, Holland PR, Goadsby PJ. Diencephalic and brainstem mechanisms in migraine. Nature reviews Neuroscience. 2011; 12(10):570–584. [PubMed: 21931334]
3. Andersson, J., Jenkinson, M., Smith, S. FMRIB technical report TR07JA2. 2010. Non-linear registration, aka spatial normalisation.
4. Ayata C. Cortical spreading depression triggers migraine attack: pro. Headache. 2010; 50(4):725–730. [PubMed: 20456160]
5. Baekey DM, Molkov YI, Paton JF, Rybak IA, Dick TE. Effect of baroreceptor stimulation on the respiratory pattern: insights into respiratory-sympathetic interactions. Respir Physiol Neurobiol. 2010; 174(1–2):135–145. [PubMed: 20837166]

6. Beissner F, Baudrexel S. Investigating the human brainstem with structural and functional MRI. Front Hum Neurosci. 2014; 8:116. [PubMed: 24616692]
7. Beissner F, Meissner K, Bär K-J, Napadow V. The autonomic brain: an activation likelihood estimation meta-analysis for central processing of autonomic function. J Neurosci. 2013; 33(25): 10503–10511. [PubMed: 23785162]
8. Benarroch EE. The central autonomic network: functional organization, dysfunction, and perspective. Mayo Clin Proc. 1993; 68(10):988–1001. [PubMed: 8412366]
9. Binks AP, Banzett RB, Duvivier C. An inexpensive, MRI compatible device to measure tidal volume from chest-wall circumference. Physiol Meas. 2007; 28(2):149–159. [PubMed: 17237587]
10. Borsook D, Burstein R, Becerra L. Functional imaging of the human trigeminal system: opportunities for new insights into pain processing in health and disease. Journal of neurobiology. 2004; 61(1):107–125. [PubMed: 15362156]
11. Borsook D, Veggeberg R, Erpelding N, Borra R, Linnman C, Burstein R, Becerra L. The Insula: A "Hub of Activity" in Migraine. Neuroscientist. 2015
12. Bossut DF, Maixner W. Effects of cardiac vagal afferent electrostimulation on the responses of trigeminal and trigeminothalamic neurons to noxious orofacial stimulation. Pain. 1996; 65(1):101–109. [PubMed: 8826496]
13. Burstein R, Noseda R, Borsook D. Migraine: multiple processes, complex pathophysiology. The Journal of neuroscience : the official journal of the Society for Neuroscience. 2015; 35(17):6619–6629. [PubMed: 25926442]
14. Burstein R, Yamamura H, Malick A, Strassman AM. Chemical stimulation of the intracranial dura induces enhanced responses to facial stimulation in brain stem trigeminal neurons. J Neurophysiol. 1998; 79(2):964–982. [PubMed: 9463456]
15. Cechetto DF. Cortical control of the autonomic nervous system. Exp Physiol. 2014; 99(2):326–331. [PubMed: 24121283]
16. Chebbi R, Boyer N, Monconduit L, Artola A, Luccarini P, Dallel R. The nucleus raphe magnus OFF-cells are involved in diffuse noxious inhibitory controls. Experimental neurology. 2014; 256:39–45. [PubMed: 24681000]
17. Chen SP, Ay I, de Morais AL, Qin T, Zheng Y, Sadeghian H, Oka F, Simon B, Eikermann-Haerter K, Ayata C. Vagus nerve stimulation inhibits cortical spreading depression. Pain. 2016; 157(4): 797–805. [PubMed: 26645547]
18. Couto LB, Moroni CR, dos Reis Ferreira CM, Elias-Filho DH, Parada CA, Pela IR, Coimbra NC. Descriptive and functional neuroanatomy of locus coeruleus-noradrenaline-containing neurons involvement in bradykinin-induced antinociception on principal sensory trigeminal nucleus. Journal of chemical neuroanatomy. 2006; 32(1):28–45. [PubMed: 16678997]
19. Deen M, Christensen CE, Hougaard A, Hansen HD, Knudsen GM, Ashina M. Serotonergic mechanisms in the migraine brain - a systematic review. Cephalalgia. 2016
20. Dietrich S, Smith J, Scherzinger C, Hofmann-Preiss K, Freitag T, Eisenkolb A, Ringler R. A novel transcutaneous vagus nerve stimulation leads to brainstem and cerebral activations measured by functional MRI. Biomed Tech (Berl). 2008; 53(3):104–111. [PubMed: 18601618]
21. Dussor G. Serotonin, 5HT1 agonists, and migraine: new data, but old questions still not answered. Current opinion in supportive and palliative care. 2014; 8(2):137–142. [PubMed: 24670810]
22. Ellrich J, Messlinger K, Chiang CY, Hu JW. Modulation of neuronal activity in the nucleus raphe magnus by the 5-HT(1)-receptor agonist naratriptan in rat. Pain. 2001; 90(3):227–231. [PubMed: 11207394]
23. Fahy BG. Intraoperative and perioperative complications with a vagus nerve stimulation device. J Clin Anesth. 2010; 22(3):213–222. [PubMed: 20400010]
24. Frangos E, Ellrich J, Komisaruk BR. Non-invasive Access to the Vagus Nerve Central Projections via Electrical Stimulation of the External Ear: fMRI Evidence in Humans. Brain Stimulation. 2015; 8(3):624–636. [PubMed: 25573069]
25. Gao Q, Xu F, Jiang C, Chen Z, Chen H, Liao H, Zhao L. Decreased functional connectivity density in pain-related brain regions of female migraine patients without aura. Brain Res. 2016; 1632:73–81. [PubMed: 26688226]

26. Glover GH, Li TQ, Ress D. Image-based method for retrospective correction of physiological motion effects in fMRI: RETROICOR. Magn Reson Med. 2000; 44(1):162–167. [PubMed: 10893535]
27. Greicius MD, Krasnow B, Reiss AL, Menon V. Functional connectivity in the resting brain: a network analysis of the default mode hypothesis. Proc Natl Acad Sci USA. 2003; 100(1):253–258. [PubMed: 12506194]
28. Greve DN, Fischl B. Accurate and robust brain image alignment using boundary-based registration. Neuroimage. 2009; 48(1):63–72. [PubMed: 19573611]
29. Hadjikhani N, Ward N, Boshyan J, Napadow V, Maeda Y, Truini A, Caramia F, Tinelli E, Mainero C. The missing link: enhanced functional connectivity between amygdala and visceroceptive cortex in migraine. Cephalalgia. 2013; 33(15):1264–1268. [PubMed: 23720503]
30. Harriott AM, Schwedt TJ. Migraine is associated with altered processing of sensory stimuli. Current pain and headache reports. 2014; 18(11):458. [PubMed: 25245197]
31. Hayasaka S, Nichols TE. Validating cluster size inference: random field and permutation methods. Neuroimage. 2003; 20(4):2343–2356. [PubMed: 14683734]
32. Headache Classification Subcommittee of the International Headache S. The International Classification of Headache Disorders: 2nd edition. Cephalalgia. 2004; 24(Suppl 1):9–160. [PubMed: 14979299]
33. Hord ED, Evans MS, Mueed S, Adamolekun B, Naritoku DK. The effect of vagus nerve stimulation on migraines. J Pain. 2003; 4(9):530–534. [PubMed: 14636821]
34. Jenkinson M, Bannister P, Brady M, Smith S. Improved optimization for the robust and accurate linear registration and motion correction of brain images. Neuroimage. 2002; 17(2):825–841. [PubMed: 12377157]
35. Kim J, Loggia ML, Cahalan CM, Harris RE, Beissner F, Garcia RG, Kim H, Barbieri R, Wasan AD, Edwards RR, Napadow V. The somatosensory link in fibromyalgia: functional connectivity of the primary somatosensory cortex is altered by sustained pain and is associated with clinical/autonomic dysfunction. Arthritis Rheumatol. 2015; 67(5):1395–1405. [PubMed: 25622796]
36. Kiyokawa J, Yamaguchi K, Okada R, Maehara T, Akita K. Origin, course and distribution of the nerves to the posterosuperior wall of the external acoustic meatus. Anat Sci Int. 2014; 89(4):238–245. [PubMed: 24604237]
37. Kraus T, Kiess O, Hosl K, Terekhin P, Kornhuber J, Forster C. CNS BOLD fMRI effects of sham-controlled transcutaneous electrical nerve stimulation in the left outer auditory canal - a pilot study. Brain Stimul. 2013; 6(5):798–804. [PubMed: 23453934]
38. Kurth F, Zilles K, Fox PT, Laird AR, Eickhoff SB. A link between the systems: functional differentiation and integration within the human insula revealed by meta-analysis. Brain structure & function. 2010; 214(5–6):519–534. [PubMed: 20512376]
39. Lance JW, Lambert GA, Goadsby PJ, Duckworth JW. Brainstem influences on the cephalic circulation: experimental data from cat and monkey of relevance to the mechanism of migraine. Headache. 1983; 23(6):258–265. [PubMed: 6643036]
40. Lee J, Lin RL, Garcia RG, Kim J, Kim H, Loggia ML, Mawla I, Wasan AD, Edwards RR, Rosen BR, Hadjikhani N, Napadow V. Reduced insula habituation associated with amplification of trigeminal brainstem input in migraine. Cephalalgia. 2016
41. Levy D, Jakubowski M, Burstein R. Disruption of communication between peripheral and central trigeminovascular neurons mediates the antimigraine action of 5HT 1B/1D receptor agonists. Proc Natl Acad Sci U S A. 2004; 101(12):4274–4279. [PubMed: 15016917]
42. Llorca-Torralba M, Borges G, Neto F, Mico JA, Berrocoso E. Noradrenergic Locus Coeruleus pathways in pain modulation. Neuroscience. 2016
43. Lyubashina OA, Sokolov AY, Panteleev SS. Vagal afferent modulation of spinal trigeminal neuronal responses to dural electrical stimulation in rats. Neuroscience. 2012; 222:29–37. [PubMed: 22800563]
44. Magis D. Neuromodulation in migraine: state of the art and perspectives. Expert Rev Med Devices. 2015; 12(3):329–339. [PubMed: 25633885]

45. Mainero C, Boshyan J, Hadjikhani N. Altered functional magnetic resonance imaging resting-state connectivity in periaqueductal gray networks in migraine. Ann Neurol. 2011; 70(5):838–845. [PubMed: 22162064]
46. Miyazaki M, Arata A, Tanaka I, Ezure K. Activity of rat pump neurons is modulated with central respiratory rhythm. Neurosci Lett. 1998; 249(1):61–64. [PubMed: 9672389]
47. Miyazaki M, Tanaka I, Ezure K. Excitatory and inhibitory synaptic inputs shape the discharge pattern of pump neurons of the nucleus tractus solitarii in the rat. Exp Brain Res. 1999; 129(2): 191–200. [PubMed: 10591893]
48. Mosqueira AJ, Lopez-Manzanares L, Canneti B, Barroso A, Garcia-Navarrete E, Valdivia A, Vivancos J. Vagus nerve stimulation in patients with migraine. Rev Neurol. 2013; 57(2):57–63. [PubMed: 23836335]
49. Moulton EA, Becerra L, Johnson A, Burstein R, Borsook D. Altered hypothalamic functional connectivity with autonomic circuits and the locus coeruleus in migraine. PLoS ONE. 2014; 9(4):e95508. [PubMed: 24743801]
50. Moulton EA, Burstein R, Tully S, Hargreaves R, Becerra L, Borsook D. Interictal dysfunction of a brainstem descending modulatory center in migraine patients. PLoS ONE. 2008; 3(11):e3799. [PubMed: 19030105]
51. Naidich, TP., Duvernoy, HM., Delman, BN., Sorensen, AG., Kollias, SS., Haacke, EM. Duvernoy's Atlas of the Human Brain Stem and Cerebellum. Vienna: Springer Vienna; 2009.
52. Napadow V, Dhond R, Park K, Kim J, Makris N, Kwong KK, Harris RE, Purdon PL, Kettner N, Hui KK. Time-variant fMRI activity in the brainstem and higher structures in response to acupuncture. Neuroimage. 2009; 47(1):289–301. [PubMed: 19345268]
53. Napadow V, Edwards RR, Cahalan CM, Mensing G, Greenbaum S, Valovska A, Li A, Kim J, Maeda Y, Park K, Wasan AD. Evoked pain analgesia in chronic pelvic pain patients using respiratory-gated auricular vagal afferent nerve stimulation. Pain Med. 2012; 13(6):777–789. [PubMed: 22568773]
54. Nichols TE, Holmes AP. Nonparametric permutation tests for functional neuroimaging: a primer with examples. Hum Brain Mapp. 2002; 15(1):1–25. [PubMed: 11747097]
55. Niddam DM, Lai KL, Fuh JL, Chuang CY, Chen WT, Wang SJ. Reduced functional connectivity between salience and visual networks in migraine with aura. Cephalalgia. 2016; 36(1):53–66. [PubMed: 25888585]
56. Nomura S, Mizuno N. Central distribution of primary afferent fibers in the Arnold's nerve (the auricular branch of the vagus nerve): a transganglionic HRP study in the cat. Brain Res. 1984; 292(2):199–205. [PubMed: 6692153]
57. Norgren R. Projections from the nucleus of the solitary tract in the rat. Neuroscience. 1978; 3(2): 207–218. [PubMed: 733004]
58. Noseda R, Burstein R. Migraine pathophysiology: anatomy of the trigeminovascular pathway and associated neurological symptoms, CSD, sensitization and modulation of pain. Pain. 2013; 154(Suppl 1)
59. Noseda R, Jakubowski M, Kainz V, Borsook D, Burstein R. Cortical projections of functionally identified thalamic trigeminovascular neurons: implications for migraine headache and its associated symptoms. The Journal of neuroscience : the official journal of the Society for Neuroscience. 2011; 31(40):14204–14217. [PubMed: 21976505]
60. Ossipov MH, Morimura K, Porreca F. Descending pain modulation and chronification of pain. Current opinion in supportive and palliative care. 2014; 8(2):143–151. [PubMed: 24752199]
61. Peuker ET, Filler TJ. The nerve supply of the human auricle. Clin Anat. 2002; 15(1):35–37. [PubMed: 11835542]
62. Ramirez Rosas MB, Labruijere S, Villalon CM, Maassen Vandenbrink A. Activation of 5-hydroxytryptamine1B/1D/1F receptors as a mechanism of action of antimigraine drugs. Expert opinion on pharmacotherapy. 2013; 14(12):1599–1610. [PubMed: 23815106]
63. Richter F, Mikulik O, Ebersberger A, Schaible HG. Noradrenergic agonists and antagonists influence migration of cortical spreading depression in rat-a possible mechanism of migraine prophylaxis and prevention of postischemic neuronal damage. Journal of cerebral blood flow and

metabolism : official journal of the International Society of Cerebral Blood Flow and Metabolism. 2005; 25(9):1225–1235.

64. Saper CB. The central autonomic nervous system: conscious visceral perception and autonomic pattern generation. Annu Rev Neurosci. 2002; 25:433–469. [PubMed: 12052916]
65. Schoenen J, Roberta B, Magis D, Coppola G. Noninvasive neurostimulation methods for migraine therapy: The available evidence. Cephalalgia. 2016
66. Schulte LH, May A. The migraine generator revisited: continuous scanning of the migraine cycle over 30 days and three spontaneous attacks. Brain. 2016; 139(Pt 7):1987–1993. [PubMed: 27190019]
67. Schwedt TJ, Chiang CC, Chong CD, Dodick DW. Functional MRI of migraine. The Lancet Neurology. 2015; 14(1):81–91. [PubMed: 25496899]
68. Seeley WW, Menon V, Schatzberg AF, Keller J, Glover GH, Kenna H, Reiss AL, Greicius MD. Dissociable intrinsic connectivity networks for salience processing and executive control. The Journal of neuroscience : the official journal of the Society for Neuroscience. 2007; 27(9):2349–2356. [PubMed: 17329432]
69. Smith SM. Fast robust automated brain extraction. Hum Brain Mapp. 2002; 17(3):143–155. [PubMed: 12391568]
70. Smitherman TA, Burch R, Sheikh H, Loder E. The prevalence, impact, and treatment of migraine and severe headaches in the United States: a review of statistics from national surveillance studies. Headache. 2013; 53(3):427–436. [PubMed: 23470015]
71. Stankewitz A, Aderjan D, Eippert F, May A. Trigeminal nociceptive transmission in migraineurs predicts migraine attacks. The Journal of neuroscience : the official journal of the Society for Neuroscience. 2011; 31(6):1937–1943. [PubMed: 21307231]
72. Straube A, Ellrich J, Eren O, Blum B, Ruscheweyh R. Treatment of chronic migraine with transcutaneous stimulation of the auricular branch of the vagal nerve (auricular t-VNS): a randomized, monocentric clinical trial. J Headache Pain. 2015; 16:543. [PubMed: 26156114]
73. Takahashi T, Shirasu M, Shirasu M, Kubo KY, Onozuka M, Sato S, Itoh K, Nakamura H. The locus coeruleus projects to the mesencephalic trigeminal nucleus in rats. Neuroscience research. 2010; 68(2):103–106. [PubMed: 20599446]
74. Van Bockstaele EJ, Peoples J, Telegan P. Efferent projections of the nucleus of the solitary tract to peri-locus coeruleus dendrites in rat brain: evidence for a monosynaptic pathway. J Comp Neurol. 1999; 412(3):410–428. [PubMed: 10441230]
75. Van Dijk KRA, Hedden T, Venkataraman A, Evans KC, Lazar SW, Buckner RL. Intrinsic functional connectivity as a tool for human connectomics: theory, properties, and optimization. J Neurophysiol. 2010; 103(1):297–321. [PubMed: 19889849]
76. Ventureyra EC. Transcutaneous vagus nerve stimulation for partial onset seizure therapy. A new concept Childs Nerv Syst. 2000; 16(2):101–102. [PubMed: 10663816]
77. Wang QP, Nakai Y. The dorsal raphe: an important nucleus in pain modulation. Brain Res Bull. 1994; 34(6):575–585. [PubMed: 7922601]
78. Woolrich MW, Jbabdi S, Patenaude B, Chappell M, Makni S, Behrens T, Beckmann C, Jenkinson M, Smith SM. Bayesian analysis of neuroimaging data in FSL. Neuroimage. 2009; 45(1 Suppl):S173–186. [PubMed: 19059349]
79. Xue T, Yuan K, Cheng P, Zhao L, Zhao L, Yu D, Dong T, von Deneen KM, Gong Q, Qin W, Tian J. Alterations of regional spontaneous neuronal activity and corresponding brain circuit changes during resting state in migraine without aura. NMR in biomedicine. 2013; 26(9):1051–1058. [PubMed: 23348909]
80. Yuan H, Silberstein SD. Vagus Nerve Stimulation and Headache. Headache. 2015
81. Yuan H, Silberstein SD. Vagus Nerve and Vagus Nerve Stimulation, a Comprehensive Review: Part I. Headache. 2016; 56(1):71–78. [PubMed: 26364692]
82. Zhou Z, Champagnat J, Poon CS. Phasic and long-term depression in brainstem nucleus tractus solitarius neurons: differing roles of AMPA receptor desensitization. J Neurosci. 1997; 17(14):5349–5356. [PubMed: 9204919]

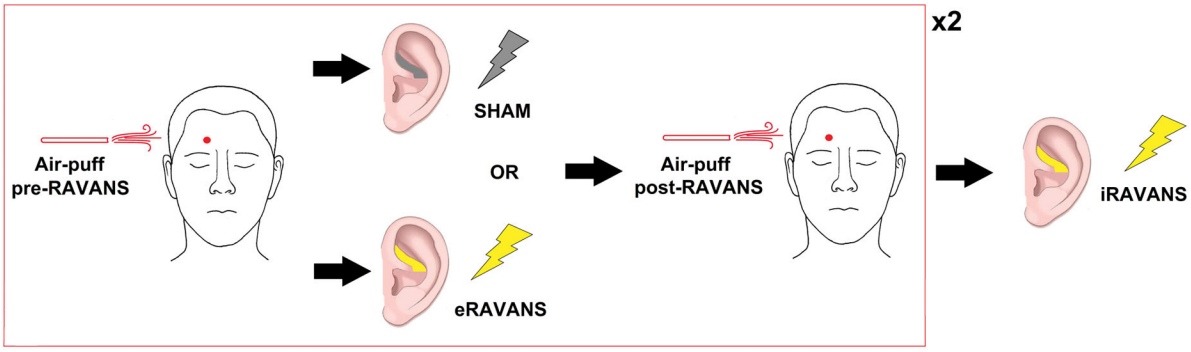

Figure 1.
Overview of our cross-over experimental design.

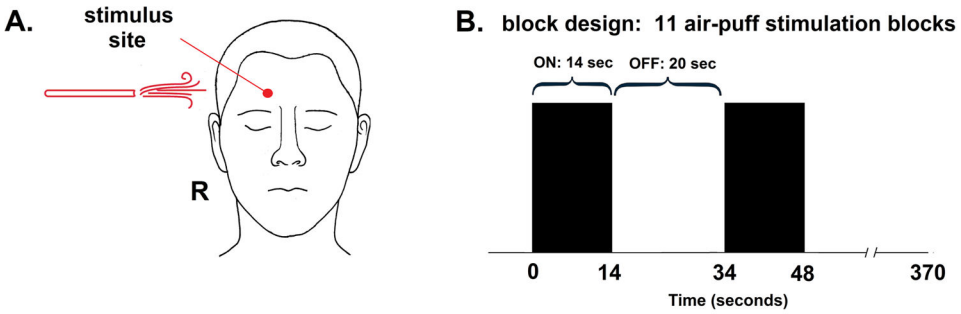

Figure 2.

Tactile somatosensory (air-puff) stimulation during fMRI was completed pre- and post-eRAVANS and SHAM stimulation. (A) right forehead (V_1, ophthalmic nerve territory) was stimulated (B) in a block design (air pressure = 80 Psi with 5 Hz, 11 repetitions, 14-second stimulation blocks alternating with 20-second rest blocks).

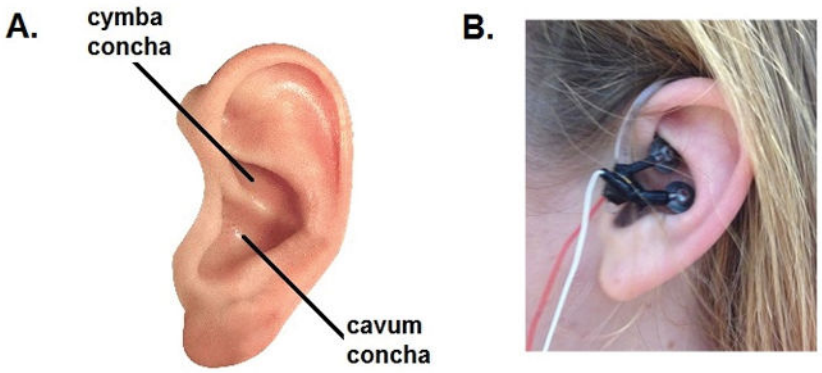

Figure 3.
(A) Schematic showing location of cymba concha and cavum concha in the auricle. (B) MR-compatible electrode placement for RAVANS.

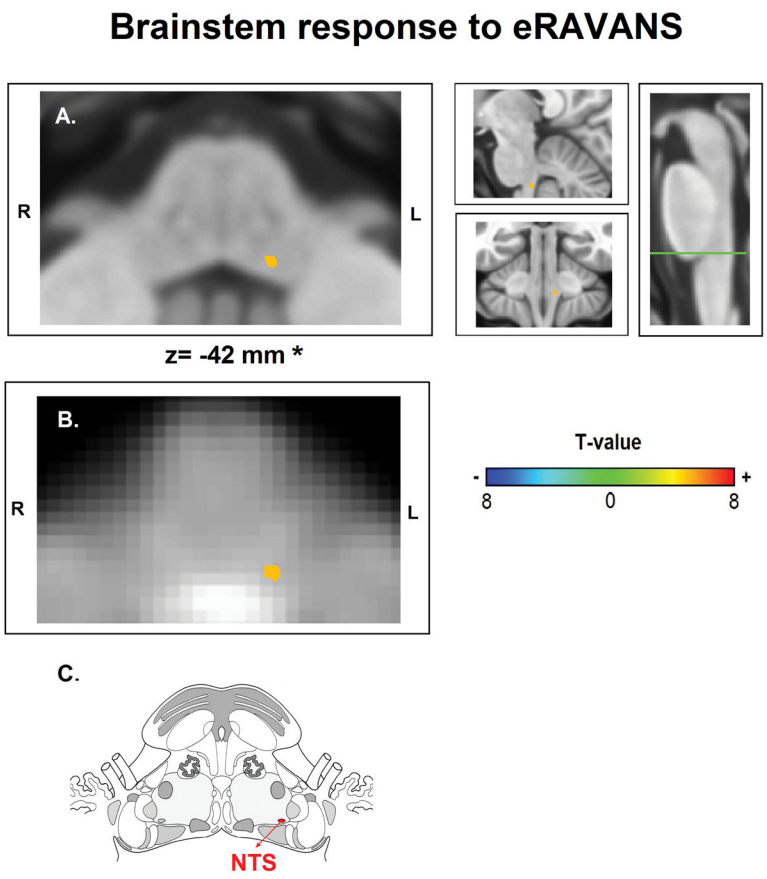

Figure 4.

FMRI brainstem response to Respiratory-gated Auricular Vagal Afferent Nerve Stimulation (RAVANS). Activation found in the left nucleus tractus solitarius (NTS) when contrasting RAVANS vs SHAM stimulation overlayed on (A) MNI-space template and (B) group-averaged functional images rotated for consistency with (C) the Duvernoy brainstem atlas. Right panel of (A) shows the level of the axial slice in green (Obex+18 mm) and sagittal and coronal views of NTS activation. *z-coordinates refer to MNI space results and not the particular image visualized.

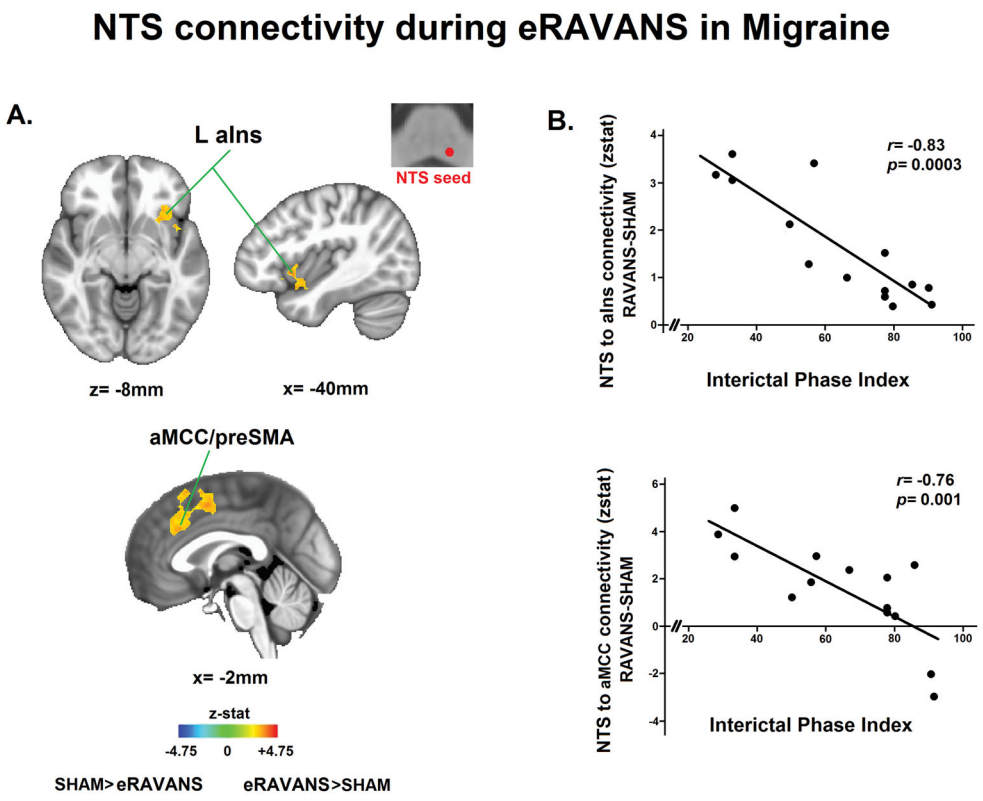

Figure 5.

Functional connectivity from left nucleus tractus solitarii (NTS) to higher brain regions in response to RAVANS stimulation. (A) Difference maps contrasting functional NTS connectivity during RAVANS versus SHAM stimulation noted increased connectivity in left anterior insula (aIns), left anterior mid-cingulate cortex (aMCC) and pre-supplementary motor area (preSMA) in migraine patients. (B) Correlation between NTS connectivity (eRAVANS-SHAM) to regions found in (A) and interictal phase at the time of the scan (a relative ratio between preceding and subsequent attacks). Greater interictal phase index was correlated with lower NTS connectivity to aIns and aMCC – i.e. NTS connectivity with cortical regions was reduced as migraine subjects approached their next migraine attack. HC=healthy controls. MIG=migraine patients.

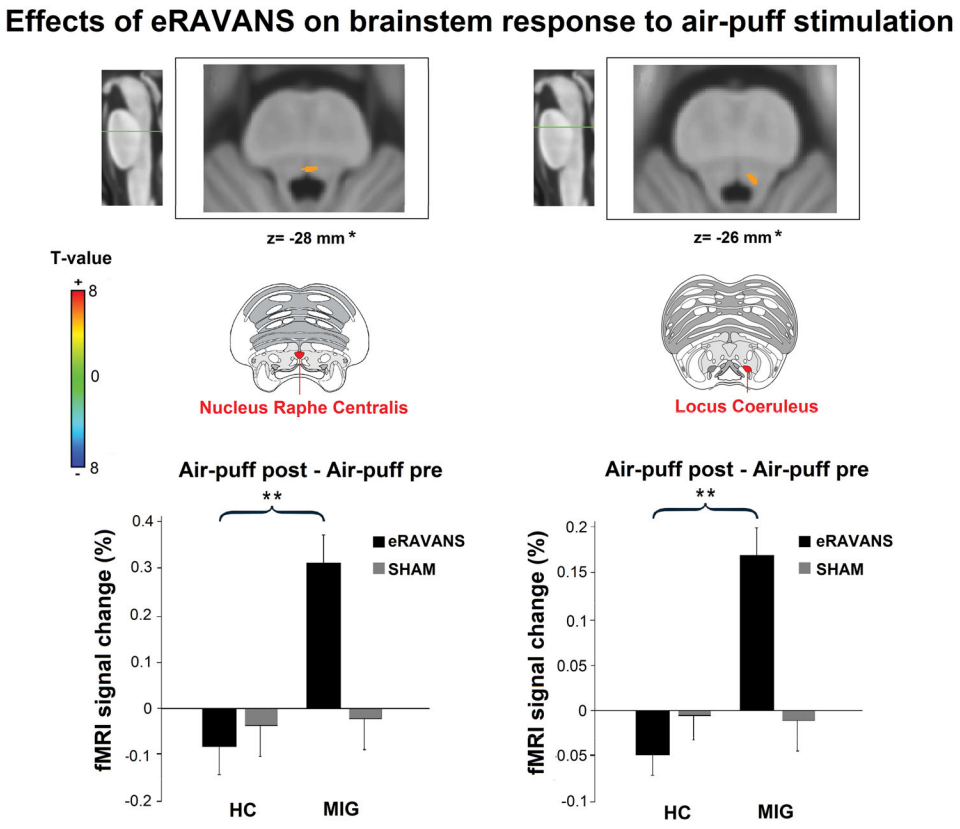

Figure 6.

Post-stimulus effects of eRAVANS on brainstem response to tactile (air-puff) trigeminal sensory stimulation. eRAVANS increased activation to air-puff stimulation in nucleus raphe centralis (Obex+32 mm) and left locus coeruleus (Obex+34 mm). Images are overlayed on MNI-space template rotated for consistency with the Duvernoy brainstem atlas. Increased nucleus raphe centralis and locus coeruleus activity after eRAVANS vs SHAM was significantly greater in migraine subjects compared to healthy controls. HC=healthy controls. MIG=migraine patients. ** $p<0.01$. Plot error bars denote standard error of the mean. *z-coordinates refer to MNI space results and not the particular image visualized.

Table 1

Demographic characteristics and clinical features of migraine patients and healthy controls.

	Healthy Controls (HC, n=16)		Migraine Patients (MIG, n=16)		*p*-value (HC vs. MIG)
	Mean±SD	**Min – Max**	**Mean±SD**	**Min –Max**	
Demographics					
Age (years old)	36.0±13.7	18–59	35.8±13.4	19 – 59	0.96
Clinical measures					
Preceding attack (days)	n/a	n/a	6.12±5.77	1 – 21	n/a
Next attack (days)	n/a	n/a	3.81±5.56	0 – 24	n/a
Interictal phase index (0–100)	n/a	n/a	63.09±27.18	4 – 100	n/a
Migraine Duration (years)	n/a	n/a	14.91±13.00	1 – 44	n/a
Episodes per month	n/a	n/a	5.88±2.63	2 – 12	n/a
Psychophysics					
eRAVANS current intensity (mA)	1.22±1.33	0.5 – 3.8	0.97±1.12	0.54 – 2.8	0.22
iRAVANS current intensity (mA)	0.85±1.07	0.49 – 2.6	1.04±1.37	0.46 – 3.5	0.36
Number of breaths - eRAVANS	90.4±15.4	72 – 117	91.3±17.4	68–118	0.87
Number of breaths - iRAVANS	94.5±18.9	77 – 118	90.2±12.9	68 – 109	0.46
Number of breaths - SHAM	90.1±15.5	66 – 121	95.7±17.6	76 – 119	0.35
Pre-eRAVANS air-puff intensity (0–10, NRS)	3.31±1.74	1 – 9	3.63±1.75	1 – 8	0.63
Post-eRAVANS air-puff intensity (0–10, NRS)	3.12±2.21	1 – 9	3.53±2.01	1 – 8	0.59
Pre-SHAM air-puff intensity (0–10, NRS)	3.31±1.70	1 – 6	3.68±2.02	1 – 9	0.57
Post-SHAM air-puff intensity (0–10, NRS)	3.18±1.83	1 – 8	3.46±1.92	1 – 8	0.67

Data are shown as mean±SD (minimum-maximum). Interictal phase index = ratio between preceding (=0) and subsequent (=100) attacks from experiment visit. NRS = numerical rating scale (0: no sensation, 10: pain detection threshold). n/a = not applicable.

Table 2

List of prophylactic medications received by subjects in the study.

Prophylactic Medication	Number of subjects
Beta-blockers	
Propranolol	2
Atenolol	1
Tricyclic antidepressants	
Amitriptyline	2
Nortriptyline	1
Topiramate	1

Table 3

Brainstem response and connectivity to RAVANS

A-Brainstem response to eRAVANS versus SHAM stimulation (all subjects included, MIG+HC)							
			MNI coordinates (mm)			**Obex (mm)**	**Peak T-value**
	Side	**Cluster Size (voxels)**	**X**	**Y**	**Z**		**eRAVANS > SHAM**
Nucleus Tractus Solitarii	L	2	−8	−38	−42	+ 18 mm	4.07
B- NTS connectivity to higher brain regions: eRAVANS versus SHAM stimulation in MIG							
			MNI coordinates (mm)			Peak Z-score		
	Side	Cluster Size (voxels)	X	Y	Z	eRAVANS >SHAM	eRAVANS	SHAM
Anterior Insula	L	529	−30	18	−6	3.14	3.04	−2.32
Mid-Cingulate Cortex	L	916	−2	26	30	3.41	2.94	−0.34
C- Effects of eRAVANS on brainstem response to tactile (air-puff) trigeminal sensory stimulation: eRAVANS vs SHAM in MIG							
			MNI coordinates (mm)			Obex (mm)	Peak T-value
	Side	Cluster Size (voxels)	X	Y	Z		eRAVANS > SHAM
Nucleus Raphe Centralis	L	3	0	−36	−28	+32	4.76
Locus Coeruleus	L		−4	−36	−26	+34	4.68